

# The Impact of PV Panel Positioning and Degradation on the PV Inverter Lifetime and Reliability

Sara Bouguerra, *Student Member, IEEE*, Mohamed Rédha Yaiche, Oussama Gassab, *Student Member, IEEE*, Ariya Sangwongwanich, *Member, IEEE*, and Frede Blaabjerg, *Fellow, IEEE*

**Abstract**— The PV inverter lifetime is affected by mission profiles, which include the solar irradiance and ambient temperature of the installation site. In previous research, the design for reliability approach has been used to evaluate the reliability of the PV inverter, where the solar irradiances have been measured on a fixed tilt and orientation angle. In most cases, the tilt is chosen to be the latitude angle and the orientation is facing south for maximum energy production throughout the year. However, the impact of the tilt and orientation of the PV array on the inverter lifetime has not been considered so far. The tradeoff between the PV energy yield and the inverter lifetime can be analysed for different PV array positioning. This paper thus evaluates the lifetime of the PV inverter with varying the tilt and orientation angle of PV panels, where the PV panel degradation rate is also taken into account. The evaluation is based on the mission profiles of Algiers, Algeria. The results reveal that orientation has a strong impact on the PV inverter loading and certain orientations result in high PV energy production and long lifetime of the PV inverter. It is also shown that the PV panel aging in Algeria has a significant impact on the lifetime estimation of the PV inverter for different orientations.

**Index Terms**—Degradation, Lifetime, Mission profile, Monte Carlo method, Orientation, PV inverters, PV panel, Reliability.

## I. INTRODUCTION

Solar photovoltaic systems (PV) have achieved grid parity in many countries, and several targets have been set to achieve 100% renewable energy systems by 2050. Moreover, it is expected that the cost of renewables will likely undercut fossil fuels in the next 10 years [1]. Solar energy is one of the most promising solutions for future energy supply. To achieve that goal, the energy harvesting from PV systems should be optimized, and this can be done by increasing the reliability of

S. Bouguerra is with the Signals and Systems Research Laboratory, Department of Electronic, Institute of Electrical and Electronics Engineering (IGEE), University M'Hamed Bougara of Boumerdes, Boumerdes, 35000, Algeria ( e-mail: s.bouguerra@univ-boumerdes.dz).

M. R. Yaiche is with Centre de Developement des Energies Renouvelable, CDER, Route de l'observatoire, Bouzaréah, 16340 Algiers, Algeria (e-mail: r.yaiche@cder.dz).

O. Gassab is with the Signals and Systems Research Laboratory, Department of Electronic, Institute of Electrical and Electronics Engineering (IGEE), University M'Hamed Bougara of Boumerdes, Boumerdes, 35000, Algeria ( e-mail: oussamagassab@yahoo.com).

A. Sangwongwanich and F. Blaabjerg are with Department of Energy Technology, Aalborg University, 9220 Aalborg, Denmark (email: ars@et.aau.dk; fbl@et.aau.dk)

power conversion systems, which are based on power electronic technology, to maximize the energy yield and reducing the system downtime. Therefore, the reliability of power electronics and lifetime estimation of power devices, used in PV converters, is an essential step to ensure high reliable operation of PV systems [2]. Solar PV systems can experience failures during the operation, which decrease their reliability and availability, and field experience revealed that power electronic components are responsible for 37% of unscheduled maintenance in the PV system [3].

Power electronics is the leading technology for the utilization of electrical energy and its conversion for different applications, renewable energies: solar and wind, individual and common transports, and power transmission. Meanwhile, many studies have been focusing on the enhancement of power electronics design and evaluation to ensure high-reliability performance, taking into account the requirement for a limited cost for market competitiveness and reduced testing time [4]. Most power converters including DC-DC converters and DC-AC converters use IGBTs as switching devices. IGBTs are among the weakest components in a PV inverter, which usually fail after a certain period [5]. The failure criteria are generally related to the increase of  $V_{ce}$  for bond wire damage, and the increase in  $R_{th}$  for solder joint fatigue (e.g. 10% for  $V_{ce}$ , 50% for  $R_{th}$ ) [6]. Reliability engineering study on power electronics is changing from handbook calculations and empirical lifetime models into the physics of failure approach [4], [7]. The PoF method identifies the failure mechanisms that cause the power device failure. In IGBTs, the main failure mechanism is bond wire fatigue [4]. The heat generated by IGBT chip during operation will cause the power module's temperature to vary rapidly, referred to as thermal cycling [8]. Due to the thermal expansion difference between bond wire and chip, the thermal cycling during operation causes bond wire fatigue due to thermo-mechanical stress [9], [10].

The reliability of power electronic devices is usually affected by external conditions, mainly solar irradiance, and ambient temperature. They are referred to as the mission profile of the system. The mission profile fluctuations create differences in the PV output power, which is translated into different switching and conduction losses in the power device, and this causes junction temperature variations during the operation [11]. Hence, the reliability of power electronic devices is

evaluated by translating the mission profile into the thermal loading of the power device using mission profile based lifetime estimation technique [6], [11-12]. In previous works, the reliability of power electronic devices is evaluated by taking into account the impacts of PV panels and the surrounding environment. In [12], the impact of the PV panel sizing on the reliability of the PV inverter is investigated, where it is revealed that the impact of PV array sizing is very high in cold climates, such as Denmark. In another study [13], the PV panel degradation is considered in the reliability analysis of the PV inverter. The results show that the estimated inverter lifetime can be deviated by 54%, due to the high degradation rate of PV panels (1% per year). In the above studies, the irradiance used in lifetime estimation is measured at certain tilt and orientation of PV panels, generally south to maximize the energy production.

The solar irradiation varies throughout the year, as the inclination of the earth's axis with respect to the sun changes throughout the year [14]. In order to receive the maximum irradiation from the sun and optimize the energy production, the tilt and orientation angles of the PV panels must be adjusted properly. The general rule for PV orientation is facing due south, in order to receive direct light from the sun by facing the equator. However, the south orientation of PV modules is not always applicable, due to geographic features and installation constraints such as shading obstructions. These aspects may change the optimal orientation of PV panels [15-16]. Several studies have investigated that the optimum tilt angle is strongly dependent on the installation site and local weather [17-19], which typically can be achieved by tilting the PV panels at the latitude angle. On the other hand, various researches [16]-[20-21] have been carried out to investigate the impact of tilt and orientation angle on the PV system performance and its economic perspective. In [16], it was found that the optimum orientation maximizing the energy production is the conventional due south or slightly west (less than 8°), while the optimum energetic tilt is slightly less than local latitude. From the economic perspective, the results revealed that the electricity cost is minimized by shifting the PV arrays west of south by 20° to 51° because the afternoon period is characterized by high peak load demand and high electricity prices, whereas the optimal economic tilt angle is also lower than local latitude to cover the summer peak demand. In another study [20], it has been investigated that the variation of tilt angles can shift the energy production from summer months to winter months, and the variation of orientation angles from east to west can shift the energy production during the day, by increasing the production in the morning or evening hours. In recent years, many PV installers claim that the variation of PV installation angles (tilt, orientation) contributes to smoothen out the feed-in tariff of PV systems, which reduces the cost in the long term. More recently in [21], it is revealed that south orientation with a tilt close to the latitude angle of the region, gives the lowest levelized cost of energy (LCOE) for that region. Besides, the south orientation also results in a high degree of autarky (DA), which is the ratio of PV directly used to the total consumption of the household. Whereas, the

combination of east and west orientations covers the midday peak, the morning consumption and reduces the cost of electricity during the night, especially in summer days. Another advantage of east and west-facing is to increase the self-consumption (SC), which is the ratio of the PV directly used to the total amount of PV generated [21-22].

Therefore, according to previous discussions, the previous works studied the impact of tilt and orientation angle on the PV energy yield and the cost, but not on the PV inverter lifetime, and this is what is going to be studied in this paper. For instance, PV panels in the same location can generally be installed with different tilt and orientation angles, which will affect the energy yield of the PV system as well as the loading and reliability of the inverter. Moreover, as discussed in [13], the reliability analysis of the PV inverter cannot be very accurate, without considering the PV panel degradation rate of the location in interest. Several studies have reported that the PV panel degradation rate in Algeria varies from 0.5% per year to 1.75 % per year as will be discussed in this paper.

In this paper, the impact of the PV panel positioning (tilt, orientation) and PV panel degradation on the PV inverter lifetime and reliability is investigated using mission profile based lifetime estimation [23]. The evaluation is based on the mission profile of Algiers, Algeria, where the irradiance values are obtained for different tilt and orientation angles. The paper is organized as follows: in Section II, a description of the case study is provided, including the mission profile of the system, tilt, and orientation of PV panels, and PV degradation studies. In Section III, the mission profile based lifetime estimation of power devices is explained. In Section IV, the reliability assessment of the PV inverter based on Monte Carlo simulation is evaluated for different tilts and orientations. After that, in Section V, the PV panel degradation is taken into account and the reliability assessment of the PV inverter for different orientations is carried out. Finally, some conclusions are drawn in Section VI.

## II. DESCRIPTION OF THE CASE STUDY

### A. System Description

In this section, a case study on a 5.2 kW single-phase, single-stage grid-connected PV inverter will be presented for lifetime estimation and reliability analysis of the PV inverter for several tilts and orientations. The PV system is configured according to Fig. 1, where the PV inverter and MPPT control are chosen according to [24]. The PV panel BP 365/65W is chosen, where 4 strings are connected in parallel and each string consists of 20 modules in series to achieve 5.2 kW rated power. The single-stage PV system consists of a full-bridge PV inverter as an interface between the PV panels and the ac grid. Transformerless PV inverters are commonly used to increase the efficiency of the PV system [23]. The 600-V/30-A IGBT and diode devices from a leading manufacturer [25] are used. The thermal parameters of the thermal impedance  $Z_{thj-c}$  for the diode and IGBT, are entered to PLECS software from the manufacturer datasheet, the parameters are given in Table I. A cooling system including the heat sink sizing is chosen to

ensure a maximum junction temperature of 120°C at the rated operating condition.

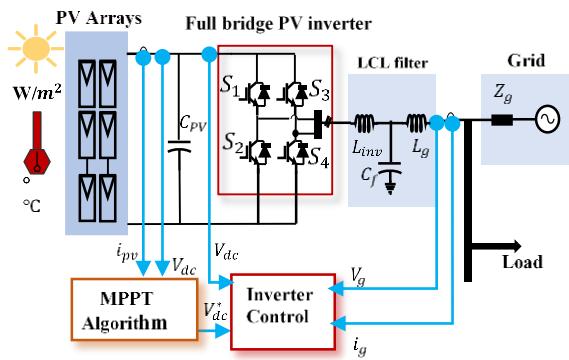


Fig. 1. Single-phase transformerless inverter with LCL filter.

TABLE I  
THERMAL IMPEDANCE PARAMETERS FOR A 600V/30A IGBT AND DIODE MODULE [25]

Thermal Impedance		$Z_{thj-c}$			
	i	1	2	3	4
IGBT	$R_{thi}$ (K/W)	0.05279	0.1938	0.2578	0.2957
	$\tau_i$ (s)	6.5e-05	0.00047	0.0061	0.06478
Diode	$R_{thi}$ (K/W)	0.037	0.237	0.5872	0.5384
	$\tau_i$ (s)	7.4e-06	7.2e-05	0.00049	0.0039

### B. Mission Profile of the PV system

The yearly solar irradiance and ambient temperature profiles are recorded from the installation site of the Algerian renewable energy development center (CDER) in Bouzaréah, Algiers with a sampling frequency of 5 minutes per sample, as it is shown in Fig. 2. The maximum and minimum temperatures are given by 35.37°C in July and 1.85°C in February, respectively, while the maximum solar irradiance throughout the year is 1293  $W/m^2$  in February. The solar irradiance is received on a south-facing, tilted plane of 36.8°, which is the latitude angle of Bouzaréah region in Algiers.

### C. Tilt and Orientation of PV Panels

The amount of irradiance the PV module collects depends on the tilt and orientation angle of the module. The tilt angle is the angle between the solar module plane and the horizontal while the orientation of the PV module is the angle between due south and the normal projection (vertical) of the solar module and horizontal. The exact tilt angle for maximum energy production varies according to the local climate and the geographic location as discussed previously, but the general rule is fixing the tilt angle at the latitude of the location plus 15 degrees in winter or minus 15 degrees in summer [26]. Nevertheless, recently solar contractors advise fixing the tilt of rooftop PV installation close or equal to the latitude angle. The optimum

orientation is usually suggested to be south-facing in the northern hemisphere and north-facing for the southern hemisphere [14]. The solar azimuth angle is the angular displacement from due south to the projection of the beam radiation on the horizontal plane, east of south is a negative angle, west is positive [26]. The tilt angle ( $\beta$ ) and azimuth angle ( $\alpha$ ) are shown in Fig. 3 [27].

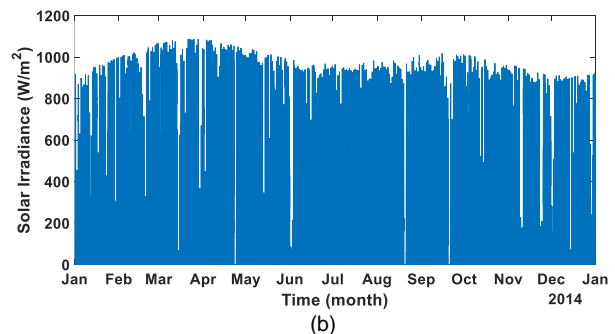
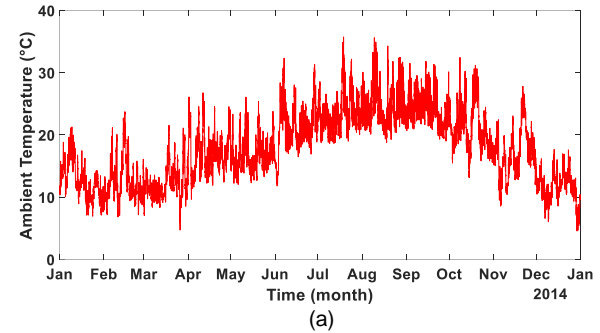


Fig. 2. Yearly mission profile data (ie, ambient temperature and irradiance with sampling rate of 5 minutes per sample) in Algeria: (a) Ambient temperature and (b) Solar irradiance with south facing and tilt of 36.8°.

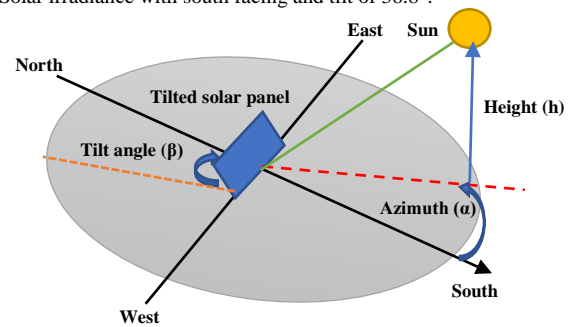


Fig. 3. Azimuth and tilt angles of a solar panel [27].

In [28], solar maps presenting the average annual global irradiation covering Algeria country is realized based on annual sunshine durations and large database. In the previous study, the global irradiation is estimated at different orientations and tilt angles, in the solar maps, it can be noticed that the highest average global irradiation is received at a tilt angle close to the latitude angle facing south.

The center of development for renewable energies (CDER) in Bouzaréah, Algiers is equipped with a meteorological station, where the global irradiances for the horizontal and tilted plane of 36.8° are measured using two Kipp and Zonen pyranometers. For this location, the latitude is 36.8° north, longitude 3.17° east and the altitude is 347 m.

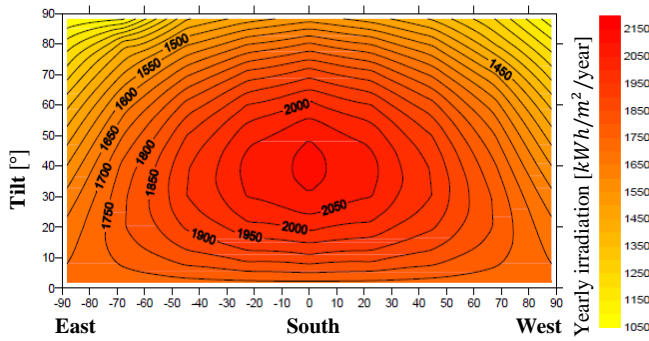


Fig. 4. Global annual solar irradiation on tilted and oriented PV modules in Bouzaréah, Algeria (N 36.8°, E 3°).

The annual total global solar irradiations for differently oriented PV panels with different tilt angles for Bouzaréah region are shown in Fig. 4 and another graph showing irradiations received on tilted planes from 0° to 90° and facing the basic orientations in this particular site is shown in Fig. 5. According to the annual irradiation levels, the optimum annual global irradiation, which is 2150 kWh/m<sup>2</sup> occurs with southern alignment and a 36° to 40° tilt angle.

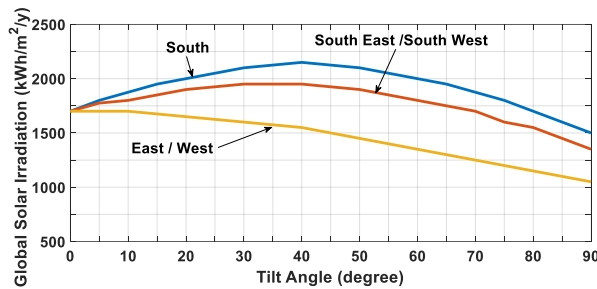


Fig. 5. Global annual solar irradiations on tilted planes with orientations of South, Southeast/Southwest, East/West for Bouzaréah, Algeria (N 36.8°, E 3°).

The global tilted irradiance for 5 different tilt angles: 20°, 30°, 37°, 50°, and 90° is obtained from the measured global horizontal irradiance using Liu and Jordan model [29]. For this study, a program for calculating the irradiance for different tilt and orientation angles, developed in CDER, is used [30]. In this program, the measured global horizontal irradiance with a sampling rate of 5 minutes is entered, with the day of the year. Then, Liu & Jordan model is used to calculate global solar irradiance for different tilt and orientations of PV panels, with high precision. The results of global solar irradiance for different tilt angles can be observed for 3 days in different seasons, as shown in Fig. 6. Then, results for different orientation angles are shown in Fig. 7. It can be noticed from Fig. 6 that the optimum tilt angle varies throughout the year, in winter the highest tilt angle (50°) is optimum (because the sun is lower in the sky) and in summer the lowest angle (20°) gives the highest irradiance level. In Algiers, Algeria, the PV panels are usually tilted at 25° to favor energy production in summer [31]. In Fig. 7, it can be noticed that the optimum orientation for maximizing the irradiance level is due south, where the maximum irradiance is seen in midday time. On the other hand,

east and west orientations give the highest irradiance levels in the morning and evening times respectively, it can be also observed that east orientation gives high irradiance levels compared to west orientation, especially in summer.

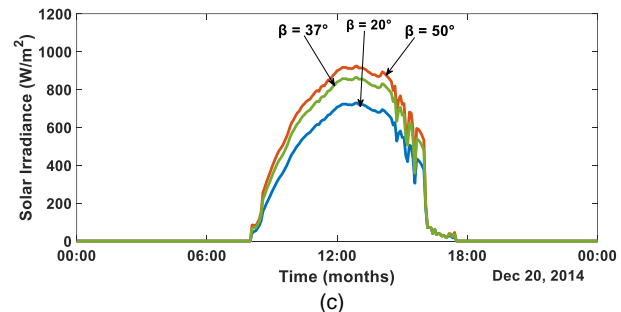
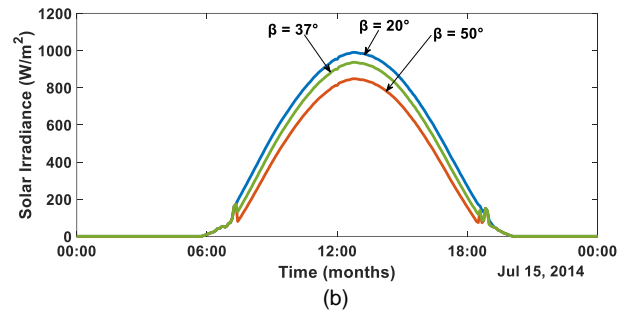
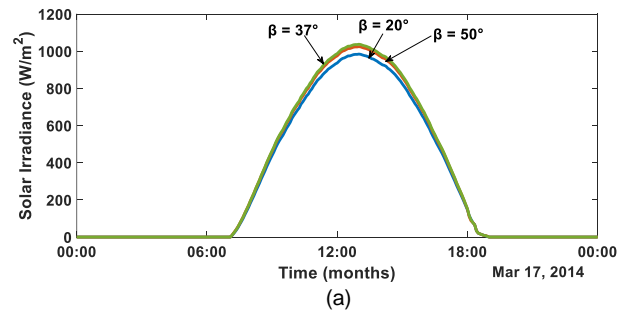


Fig. 6. Solar irradiance for 3 days in Algeria, with a sampling rate of 5 minutes per sample, for 3 different tilt angles 20°, 37° and 90° with South orientation: (a) Spring, (b) Summer, (c) Winter

#### D. PV Panel Degradation

The PV module is an essential part of the PV system since it converts the incident irradiation from the sun to electrical power for daily use, and the PV module represents more than 50% of the total cost of PV system installation [32]. In practice, the qualified PV modules usually degrade more than the rates given by the manufacturer [33-35]. The main degradation modes observed in PV modules are due to the degradation of packaging materials, loss of adhesion, degradation caused by moisture, and semiconductor device failure. The degradation of packaging material includes encapsulant browning [33]. Several works are carried out to study the aging process of EVA encapsulant in the real field [32]-[36-37]. It is revealed that this aging mechanism is the most critical and leads to PV module aging in Algeria, especially in the desert region with a hot and dry climate condition. In [38], the electrical and thermal performance of PV modules in the Algerian desert is carried out. It has been revealed that after 20 years of exposure, the PV module maximum power degraded by 35% which means 1.75%

per year.

PV modules do not frequently fail catastrophically, but they experience a steady power degradation over time. Mainly, the degradation of PV modules undergo 2 different stages, rapid degradation (1-3%) in the first year of operation then slow linear degradation (0.5% to 1% per year) thereafter [39], [40]. It is reported that PV modules mainly affected by encapsulant discoloration undergo linear degradation over time, while other degradation modes lead to non-linear degradation [41]. In [31], degradation of power performance of 90 crystalline silicon PV modules is evaluated after 11 years of exposure in the Bouzaréah region in Algeria, where the panels were divided into 3 subgroups. It has been found that the average yearly degradation rate of these modules in the Bouzaréah region in Algeria is given by 0.55% per year.

In this paper, a linear degradation model based on the measurements in [31] is proposed, since the study is evaluated using the mission profile of the same geographic location. The PV panel degradation impact is considered in Section V.

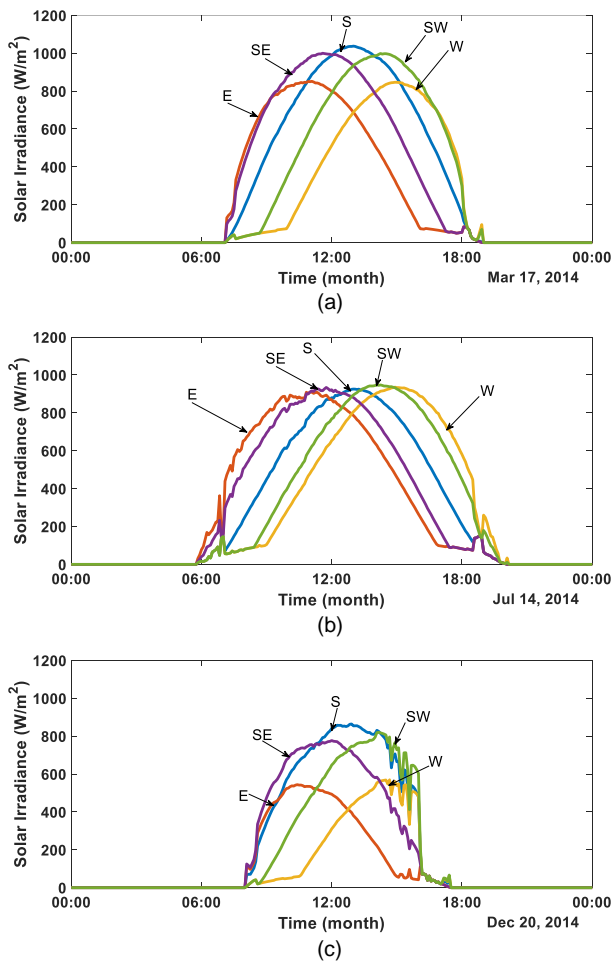


Fig. 7. Solar irradiance for 3 days in Algeria, with a sampling rate of 5 minutes per sample, for 5 different orientation angles with tilt angle is 36.8°: (a) Spring, (b) Summer, (c) Winter.

### III. MISSION PROFILE BASED LIFETIME ESTIMATION

#### A. Mission Profile Translation

The mission profile (solar irradiance, ambient temperature) for different orientations and tilt angles in Algiers are translated into thermal loading of the PV inverter. First, the grid-connected PV system in Fig. 1 is constructed in PLECS software. Then, the thermal model of the IGBTs and Diodes from the manufacturer datasheet in [25] is constructed. After that, the PV power at the MPP is obtained according to the PV arrays configuration [23]. Simulation is carried out several times using 4 ambient temperatures (-5, 15, 35, 55) °C and 16 solar irradiances (0, 100... 1500) W/m². By using lookup tables,  $T_{jm}$  and  $\Delta T_j$  values are obtained for the yearly mission profile for the Algiers region in Algeria.

#### B. Cycle Counting Algorithm

After obtaining the junction temperature  $T_j$  under the yearly mission profile, a cycling counting algorithm is applied to divide the irregular thermal loading cycles into numerous regular loading. The rainflow cycle counting algorithm [42] is a technique that identifies all the thermal cycles in a variable loading history. This algorithm is developed to consider the stress-strain hysteresis loop in temperature loading history which is the physical basis of this algorithm. It means that each closed hysteresis loop represents a cycle [6], [42]. The temperature cycles have patterns that differ in the cycle amplitude and period. Hence, Rainflow cycle counting algorithm is applied to obtain regular loading ranges, from which the mean junction temperature  $T_{jm}$ , the cycle amplitude  $\Delta T_j$ , the cycle period  $t_{on}$ , and the number of cycles  $n_i$  for each regular loading can be determined, as shown in Fig. 8. These parameters can be applied to the lifetime model in order to identify the number of cycles to failure.

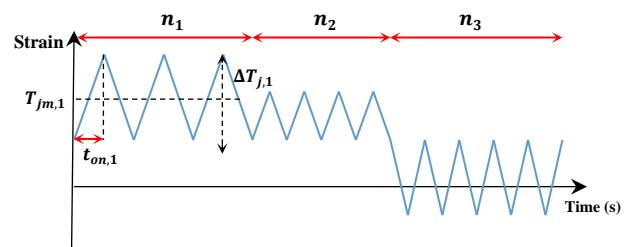


Fig. 8. Regular loading profile demonstrates the extraction of the parameters  $\Delta T_{j,i}$ ,  $T_{jm,i}$ ,  $t_{on,i}$ , and  $n_i$ .

#### C. Lifetime Model of Power devices

To predict the lifetime (cycles to failure) of the power electronic device as a function of the thermal cycling parameters, the lifetime model in [43], [44] is used. This lifetime model is derived from accelerated power cycling test data and it is given as:

$$N_f = A \cdot \Delta T_j^\alpha \cdot \exp\left(\frac{E_a}{k_b \cdot T_{jm}}\right) \cdot \alpha r^{\beta_1 \cdot \Delta T_j + \beta_0} \cdot \left(\frac{c + t_{on}^y}{c + 1}\right) \cdot f_D \quad (1)$$

where  $N_f$  is the number of cycles to failure,  $T_{jm}$  the mean junction temperature,  $\Delta T_j$  is the cycle amplitude and  $t_{on}$  is the cycle period. The lifetime model parameters include the activation energy  $E_a$ , the bond wire aspect ratio  $ar$ , the Boltzmann constant  $k_b$ , and other constants are given in Table II [44].

TABLE II  
PARAMETERS OF THE LIFETIME MODEL OF AN IGBT MODULE [44].

Parameters	Unit	Value	Experimental condition
$A$	[1]	$3.4368 \times 10^{14}$	
$\alpha$	[1]	-4.923	$64 \text{ K} \leq \Delta T_j \leq 113 \text{ K}$
$\beta_1$	[1/K]	$-9.012 \times 10^{-3}$	
$\beta_0$	[1]	1.942	$0.149 \leq ar \leq 0.42$
$C$	[1]	1.434	
$\gamma$	[1]	-1.208	$0.07 \text{ s} \leq t_{on} \leq 63 \text{ s}$
$f_D$	[1]	0.6204 for diode 1 for IGBT	$32.5 \text{ }^\circ\text{C} \leq T_j \leq 122 \text{ }^\circ\text{C}$
$E_a$	[eV]	0.06606	
$k_b$	[eV/K]	$8.6173324 \times 10^{-5}$	

#### D. Monte Carlo Simulation and Reliability Assessment

The lifetime consumption LC is calculated using Miner's rule given by:

$$LC = \sum_i \frac{n_i}{N_{fi}} \quad (2)$$

where  $n_i$  is the number of cycles, obtained by Rainflow analysis,  $N_{fi}$  is the number of cycles to failure, which is obtained from the lifetime model. The value of LC indicates how much time the device consumed during operation. If LC reaches unity ( $LC = 1$ ), then the device reaches its end of life [6]. Moreover, to overcome parameter uncertainties due to the manufacturing process and application of the lifetime model, Monte Carlo simulation is performed. In Monte Carlo simulation, two types of uncertainties are considered. The first type is parameter variation in the lifetime model because the lifetime model which has certain uncertainty due to the specific test condition. Therefore, variations should be introduced to the constants  $A$ ,  $\beta_0$  and  $\beta_1$  of the lifetime model. The second type of uncertainty is due to the manufacturing process which causes variations in the IGBT losses. In this case, variations should be introduced to the stress parameters  $T_{jm}$ ,  $\Delta T_j$  and  $t_{on}$ . To introduce these variations, the parameters are modeled with certain distribution with a range of variations. In general, the parameter variation tends to be normal distribution when the number of samples is large enough according to the central limit theorem. Thus, in this paper, the parameters are modeled with normal distribution, with certain parameter variation (e.g. 5%). After that, a large set of the population is taken randomly from each distribution. The number of simulations is selected considering the tradeoff between accuracy and computation time (e.g., 10, 000 simulations) and then the selected value is applied to the lifetime model in order to evaluate the damage accumulation [45]. The system-level reliability assessment is calculated according to the reliability block diagram [46]. For the full-bridge inverter topology (4 IGBT module components), as seen in Fig. 1, the failure of one component leads to the whole inverter system failure. Thus, the unreliability function  $F_{tot}(x)$  can be given by:

$$F_{tot}(x) = 1 - (1 - F(x))^4 \quad (3)$$

where  $F(x)$  is the unreliability function of one power device.

## IV. LIFETIME EVALUATION

### A. Translated Thermal Loading

The mission profile data for different orientations and tilt angles without PV panel degradation are translated into thermal loading of the PV inverter. When changing tilt and orientation, the ambient temperature is assumed to remain the same, and the irradiance is received at a certain tilt and orientation angle. Therefore, in this analysis, the PV power production characteristic of different panel orientations has the main influence on the thermal loading of the PV inverter, while the impact of ambient temperature (for different orientations) is less significant. This is also applied to the case where the inverter is internally housed. The impact of the tilt angle on the junction temperature profile of the IGBT device can be seen in Fig. 9. It can be observed that for south orientation, the thermal loading parameters  $T_{jm}$  and  $\Delta T_j$  are relatively high for the tilt angle of  $30^\circ$ , which is the optimum tilt angle. The thermal loading is slightly reduced with a tilt of  $20^\circ$  where  $T_{jm}$  is about  $7^\circ\text{C}$  lower, while for an inclination of  $90^\circ$  the values of  $T_{jm}$  and  $\Delta T_j$  are reduced significantly where  $T_{jm}$  is about  $25^\circ\text{C}$  lower than optimal tilt case and  $\Delta T_j$  is  $3^\circ\text{C}$  less. Besides, it can be observed that the reduction is lower in summer months, from April to September, due to the moderately stable ambient temperatures and irradiances during summertime in Algeria. This results in low cycle amplitude  $\Delta T_j$  in this period.

To illustrate the impact of orientation on the thermal loading of the PV inverter, Fig. 10 shows  $T_{jm}$  and  $\Delta T_j$  for different orientations fixing the tilt at  $37^\circ$ . It can be noticed that south orientation gives the highest thermal loading, i.e. highest  $T_{jm}$  and  $\Delta T_j$  values. On the other hand, for the east orientation,  $T_{jm}$  is less than  $3^\circ\text{C}$  lower than the south orientation. However, the thermal loading for east orientation is higher than the south orientation in summertime (from May to August) and lower during the rest of the year. The thermal loading for west orientation is slightly lower than east orientation,  $T_{jm}$  and  $\Delta T_j$  are only about  $3^\circ\text{C}$  and  $1^\circ\text{C}$  lower than the east, respectively. This slight reduction in  $T_{jm}$  and  $\Delta T_j$  is due to the decrease in irradiance levels in the evening, where the irradiance levels in the morning time are higher than evening times. In Fig. 10 (b) and Fig. 10 (d), it can be observed that the thermal loading of the power device for southeast and southwest orientations is very close to south orientation, where the differences in  $\Delta T_j$  and  $T_{jm}$  are less than  $1^\circ\text{C}$ . However, the southeast orientation is slightly higher than southwest orientation in terms of thermal loading, the highest thermal loading occurs in summer months as observed in the east and west-facing case.



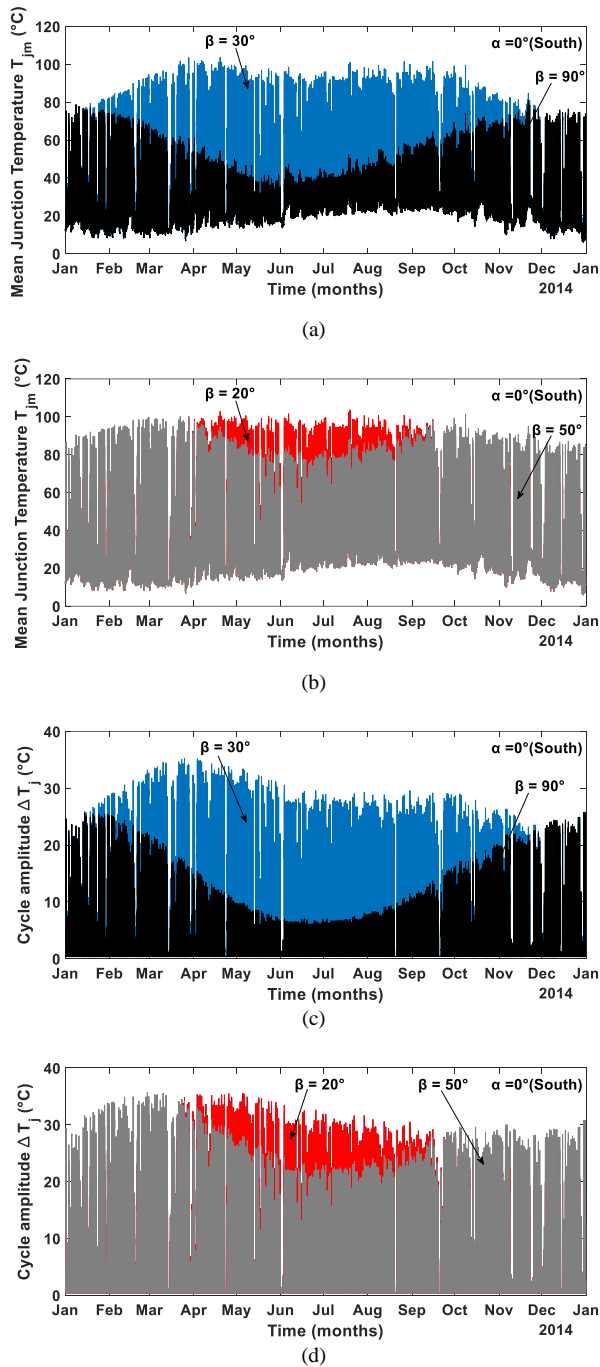


Fig. 9. Thermal loading of a single IGBT device in the PV inverter for yearly mission profile data with different tilts angles  $\beta$ : (a,b) Mean junction temperature  $T_{jm}$  and (c,d) Cycle amplitude of the junction temperature variation  $\Delta T_j$ .

### B. Lifetime Evaluation

As discussed in [45], the IGBT modules are exposed to 2 types of thermal stress, with different levels of cycling frequency. The first one is the line frequency power cycling, which comes from the variations in the IGBT power losses, due to different loading conditions. The second type is the low-frequency thermal cycling, which is caused by the variations in the ambient temperature. In order to find the lifetime consumption using Miner's rule, the number of cycles in one

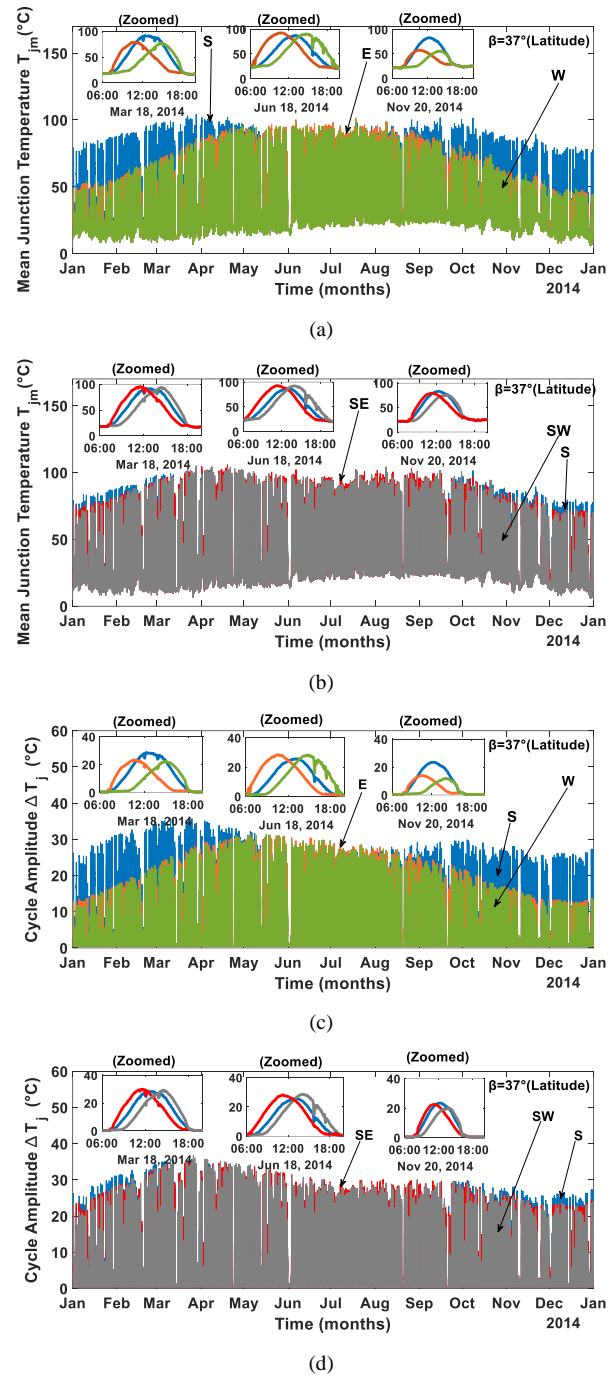


Fig. 10. Thermal loading of a single IGBT device in the PV inverter for yearly mission profile data with different Orientation angles: (a,b) Mean junction temperature  $T_{jm}$  and (c,d) Cycle amplitude of the junction temperature variation  $\Delta T_j$ .

year and the number of cycles to failure  $N_{f(line\ freq)}$  due to line frequency power cycling have to be obtained. Since the thermal loading parameters  $T_{jm}$  and  $\Delta T_j$  are obtained every 5 minutes, the number of cycles in 5 minutes have to be calculated.

$$n'_{i(line\ freq)} = 50 \times 60 \times 5 = 1.5 \times 10^4 \text{ Cycles} \quad (4)$$

The number of cycles in 5 minutes is obtained considering the number of cycles in 1s due to line frequency power cycling ( $f = 50 \text{ Hz}$ ). After that, the damage accumulation  $LC_{(line\ freq)}$  due to line frequency power cycling is calculated.

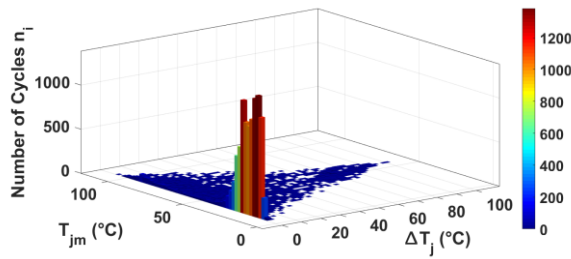


Fig. 11. Rainflow counting damage histogram of a single IGBT device with  $\alpha = 0^\circ, \beta = 37^\circ$ .

$$LC_{(line\ freq)} = n'_i{}_{(line\ freq)} \sum_i \frac{1}{N_f{}_{(line\ freq)}} \quad (5)$$

$n'_i{}_{(line\ freq)}$  is constant and  $N_f{}_{(line\ freq)}$  is a function of  $\Delta T_{ji}$  and  $T_{jmi}$  and  $t_{on}=0.01s$ , for each loading  $i$ , and it is calculated using the lifetime model in (1). The lifetime evaluation of the power device in the PV inverter is carried out for PV panels south facing with a tilt angle of  $\beta = 37^\circ$ . The damage accumulation LC due to line frequency power cycling is found to be 4.47 %, which results in an IGBT lifetime of 22 years.

On the other hand, the lifetime consumption of a single IGBT device under the high-frequency power cycling and low-frequency thermal cycling (due to mission profiles) can be obtained [47]. First, the Rainflow cycle counting algorithm is used to extract the parameters:  $T_{jmi}, \Delta T_{ji}, n_i$  and  $t_{oni}$  for each regular loading  $i$ . Then, the lifetime model in (1) is used to find the number of cycles to failure for each regular loading  $i$ . The lifetime under both effects (low and line frequency cycling) is found to be 22 years. It is worth noticing that the effect of low-frequency thermal cycling is very small and can be neglected for this case, since the damage accumulation due to the low-frequency thermal cycling is relatively low compared to the line frequency power cycling, as shown in Table III. Notably, it can be realized from Fig. 11 that the majority of thermal cycles have very low cycle amplitudes (around  $\Delta T_j = 0^\circ C$ ) and mean junction temperature less than  $30^\circ C$  ( $0^\circ C \leq T_{jm} \leq 30^\circ C$ ), and this occurs when the heating time is less than 60 s.

The lifetime evaluation of the power device is carried out for 4 different tilt angles of PV panels:  $20^\circ, 30^\circ, 50^\circ$ , and  $90^\circ$ . The results are shown in Table IV. The lifetime estimation is evaluated also for various orientations: south, southeast, southwest, east, west, and in case of splitting the PV panels equally between east/ west, and south/ west and south/east. It is worth mentioning that splitting the total installed capacity equally between east and west makes it possible to benefit from the high self-consumption of east orientation and the high degree of autarky of west orientation as done in [21]. Moreover, splitting the PV panels between south and east has the advantage of high PV energy production due to south orientation and high self-consumption of east orientation. This orientation may lead to less PV inverter loading and a higher lifetime. Whereas, splitting the total installed capacity between south and west increases the energy production with a high degree of autarky, since the customer when in evening time

which is the high consumption time directly uses the PV power, and this PV positioning may also decrease the loading the PV inverter and increase its reliability. The results of the mission profile based lifetime estimation with these different orientations are shown in Table V.

TABLE III  
DAMAGE ACCUMULATION RESULTS WITH  $\alpha = 0^\circ, \beta = 37^\circ$

Loading	Cycle period $t_{on}$	Accumulated damage LC in one year	Lifetime
Line frequency	0.01 s	$4.47 \times 10^{-2}$	22.36 years
Mission profiles (Irr and Temp)	60 s	$7.22 \times 10^{-5}$	13856 years
Total effects		$4.48 \times 10^{-2}$	22.32 years

TABLE IV  
DAMAGE ACCUMULATION RESULTS FOR DIFFERENT PV TILT ANGLES  $\alpha = 0^\circ$  (SOUTH)

Tilt Angle	Accumulated damage LC in one year	Lifetime
$20^\circ$	0.0422	24 years
$30^\circ$	0.0456	22 years
$50^\circ$	0.0371	27 years
$90^\circ$	0.0047	213 years

TABLE V  
DAMAGE ACCUMULATION RESULTS FOR DIFFERENT PV ORIENTATIONS  $\beta = 37^\circ$  (LATITUDE ANGLE)

Orientation	Accumulated damage LC in one year	Lifetime
South	0.0447	22 years
Southeast	0.0379	26 years
Southwest	0.0358	28 years
East	0.0200	50 years
West	0.0179	56 years
East + West	0.0053	187 years
South + East	0.0194	51 years
South + West	0.0185	54 years

TABLE VI  
EQUIVALENT STATIC VALUES OF THE STRESS PARAMETERS  $\alpha = 0^\circ, \beta = 37^\circ$

Parameters	Static Values
Mean junction temperature $T_{jm(static)}$	$31.92^\circ C$
Cycle amplitude $\Delta T_{j(static)}$	$18.25^\circ C$
Heating period $t_{on(static)}$	0.01 s
Number of cycles per year $n_i$	$1.577 \times 10^9$
Number of cycles to failure $N_f$	$3.53 \times 10^{10}$
Damage accumulation per year LC	0.045

In order to obtain more accurate and realistic results, parameter variations are introduced by Monte Carlo simulation and the reliability of the IGBT and the PV inverter is evaluated.



First, static values should be taken from stress parameters:  $T_{jm}$ ,  $\Delta T_j$  and  $t_{on}$  and the lifetime model constants:  $A, \beta_0, \beta_1$  as discussed in [23] and [45]. The static parameters for the orientation of south-facing and tilt angle of  $\beta=37^\circ$  are given in Table VI. After finding the static values for the different tilts and orientations, they are modeled as a normal distribution with 5% parameter variation and the simulation is repeated 10,000 times, where a random value from these static parameters is taken each time and the lifetime model is applied to obtain the damage accumulation. Finally, a histogram of end of life for a large population of IGBTs is evaluated, as shown in Fig. 12 for the case of south-facing and  $\beta=37^\circ$ . The wear-out failure of the component can usually be well represented with a Weibull distribution with an increasing failure rate over-time (when the shape parameter is larger than 1) [48]. Thus, the lifetime distribution of the power device for the different 10 000 samples is fitted with Weibull distribution in Fig. 12, whose probability density function (PDF) is given as:

$$f(x) = \frac{\beta}{\eta^\beta} x^{\beta-1} \exp\left[-\left(\frac{x}{\eta}\right)^\beta\right] \quad (6)$$

Where  $\beta$  and  $\eta$  are the shape and scale parameters respectively. The value of  $\eta$  corresponds to the time when 63.2 % of the population is failed. The unreliability function (cumulative distribution function) of the Weibull distribution is shown for one single IGBT (component level) and 4 IGBTs (full-bridge PV inverter) for the case of ( $\alpha=0^\circ, \beta=37^\circ$ ) as shown in Fig. 13.

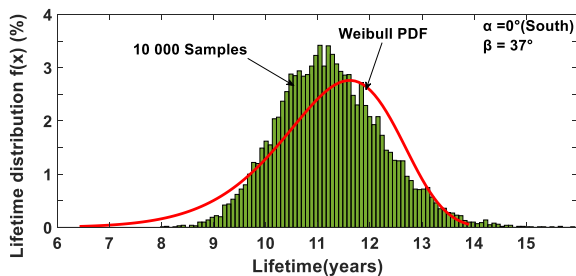


Fig. 12. Lifetime distribution of a single IGBT device in the PV inverter installed in Algeria, where the PV panels are south oriented with a tilt of  $37^\circ$ .

The unreliability function in system-level is carried out for different tilt angles of PV panels as shown in Fig. 14, and for the different orientations in Fig. 15. The  $B_x$  lifetime, the time when x% of the population of power devices is failed, can be

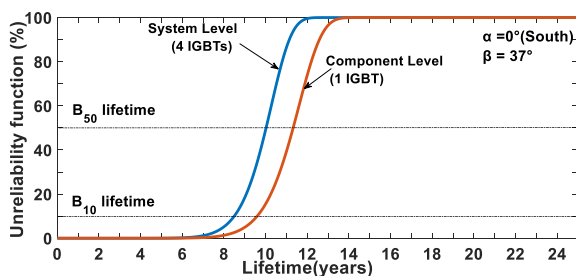


Fig. 13. Unreliability function (Weibull CDF function) of the PV inverter installed in Algeria, where the PV panels are south oriented with a tilt of  $37^\circ$ .

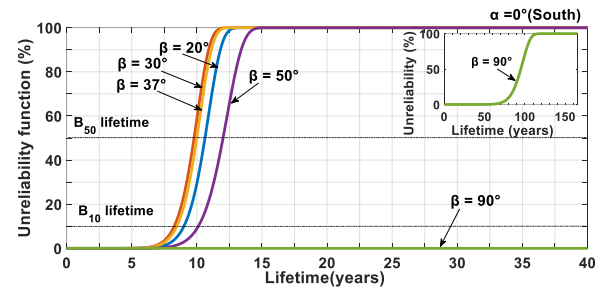


Fig. 14. Unreliability function (Weibull CDF function) of the PV inverter installed in Algeria for different tilts of PV panels oriented toward the south.

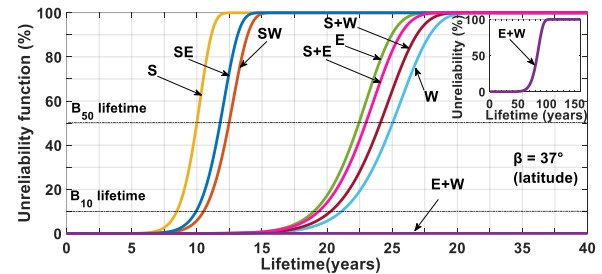


Fig. 15. Unreliability function (Weibull CDF function) of the PV inverter installed in Algeria for different orientation of PV panels tilted at the latitude angle.

obtained from the unreliability function. The PV energy production can be computed for different tilt angles and orientations of PV panels, to analyze the loss of energy production and the gain in the PV inverter lifetime ( $B_{10}$ ) when changing tilt and orientations. The results in Fig. 14 show that the tilt angle resulting in the lowest lifetime of the PV inverter is  $30^\circ$  corresponding to the highest annual energy production as can be seen in Fig. 16. However, the deviation in  $\beta_{10}$  lifetime for tilt angles of  $20^\circ, 30^\circ$ , and  $50^\circ$  is very small (less than two years) as can be observed also in Fig. 16. Moreover, the energy production is decreased by 1% for a tilt of  $20^\circ$  and 4% for a tilt of  $50^\circ$ , which means that the choice of tilt angle, less than  $20^\circ$ , around the optimum tilt does not alter the PV inverter lifetime significantly but the energy production is slightly reduced. Hence, the choice of tilt angle around the optimum is important for maximizing the energy production without affecting much the PV inverter lifetime. However, the panels tilted at  $90^\circ$ , result in a very high PV inverter lifetime, however, the PV annual energy drop is around 37%, which is a very high loss. It can be concluded that the tilt angle does not have a significant impact on the PV inverter lifetime. However, for maximizing the energy production, the careful choice of optimum tilt is mandatory.

From Fig. 15, it can be observed that the deviation in the unreliability function of the PV inverter (system level) for different PV orientations is significant, where the lowest lifetime and steepest graph corresponds to the south orientation, which is also the optimum orientation for maximizing the energy production as can be seen in Fig. 17. On the other hand, the southeast and southwest orientations result in an annual PV energy drop of 5% and 8% respectively, where the  $\beta_{10}$  lifetime gain is 17% and 24% respectively. The orientation of due east and due west lead to PV energy drop of 18% and 23%

respectively, where the  $\beta_{10}$  lifetime gain is 124% and 150% respectively. It is worth noticing that east-facing results in higher PV energy compared to west facing as discussed before, due to high irradiance levels during morning time in Algiers.

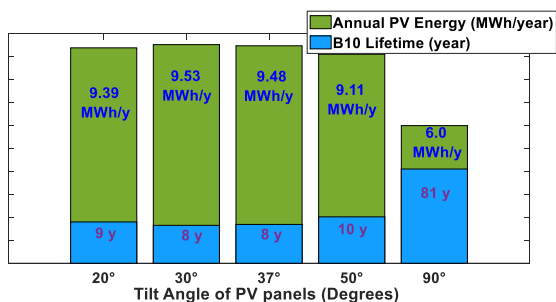


Fig. 16. PV Energy yield and  $B_{10}$  lifetime of the PV inverter installed in Algeria for different tilt angles of PV panels in one year.

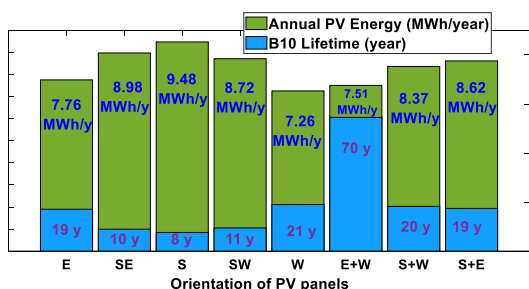


Fig. 17. PV Energy yield and  $B_{10}$  lifetime of the PV inverter installed in Algeria for different orientations of PV panels in one year.

Moreover, it can be observed that splitting the PV panels south/east and south /west result in less than 12% PV energy drop, and  $\beta_{10}$  lifetime gain of more than 130%. On the other hand, the more practical case of splitting PV capacity between east and west leads to a decrease of 20% in the annual PV energy compared to the south. The annual energy for this orientation is the average between the east and west energies, as can be visualized in Fig. 18, where the available power from PV panels is shown for 1-day operation. However, the  $\beta_{10}$  lifetime corresponding to east/west split is around 8 times the  $\beta_{10}$  for south orientation, which is very beneficial for reducing the cost of maintenance and the replacement of PV inverters. It is also worth mentioning that the orientation of due east and the case of south/east (split) result in the same PV inverter  $\beta_{10}$  lifetime (19 years) but the annual PV energy for south/east (split) is 11 % higher than east, the same remark can be said for south/west (split) and west orientation.

As can be observed in Fig. 17, the orientation of east/west split results in a very high lifetime for IGBTs, compared to the south, east or west orientations, this can make a suggestion, that this PV panel configuration drastically reduces the stress on power devices. Fig. 19 shows the thermal loading of the IGBT device for east, west and east/west (split) orientation, it can be observed that the mean junction temperature  $T_{jm}$  for E/W orientation is approximately 17°C lower than east, and 14°C lower than west orientation. On the other hand, the cycle amplitude  $\Delta T_j$  for E/W orientation is around 8°C lower than east or west. This high reduction in the thermal loading of the power

devices reduces the stress on the inverter, and the lifetime is increased considerably, as observed in Fig. 17.

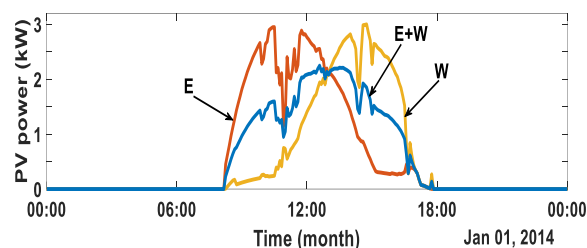
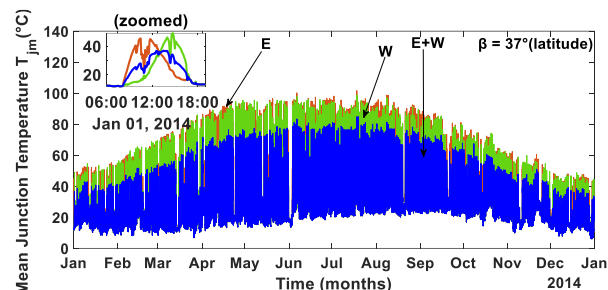
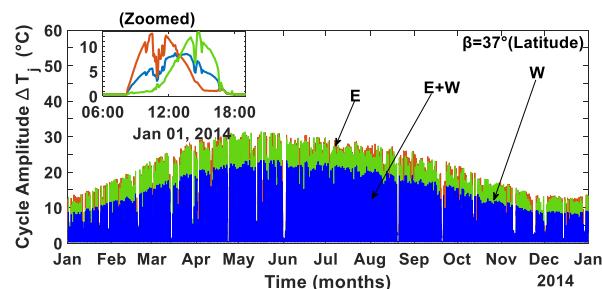


Fig. 18. Available power from PV panels in 1 day for different orientation of PV panels: East, West, E+W split.



(a)



(b)

Fig. 19. Thermal loading of a single IGBT device in the PV inverter for yearly mission profile data with different Orientation: East, West, E+W split: (a) Mean junction temperature  $T_{jm}$  and (b) Cycle amplitude of the junction temperature variation  $\Delta T_j$ .

In light of the above discussion, it can be concluded that orientation has a strong impact on the PV inverter lifetime, where the maintenance cost can be reduced significantly and the self-consumption can be increased by facing the PV panels east of south. Besides, the degree of autarky can be increased with less PV inverter loading when pointing the PV panels west of south. Furthermore, splitting the PV energy between east and west maintains the PV energy high enough with less PV inverter loading and higher lifetime (8 times higher), which results in less maintenance cost of the PV inverter during operation by replacing the inverter less often. Moreover, the initial cost of PV energy in the design phase will be much lower, and as it was investigated in several studies, the east/west orientation gives the capability of matching the load profile of the household and increases the self-consumption and degree of autarky of the PV system.

### V. LIFETIME EVALUATION CONSIDERING PV PANEL DEGRADATION

The output power of the PV arrays is obtained after an operation of 20 years, considering the PV panel degradation rate of 0.55% per year, as shown in Fig. 20. The difference in power production due to PV panel degradation can be visualized, where the available PV power decreases by 11% in 20 years. The impact of PV panel degradation can be observed in the junction temperature parameters:  $T_{jm}$  and  $\Delta T_j$ , it can be observed from Fig. 21 that the mean junction temperature  $T_{jm}$  with panel degradation of 20 years is approximately  $15^\circ$  lower than the case without PV panel degradation that corresponds to the first year of operation. On the other hand, the cycle amplitude of the junction temperature is about  $7^\circ$  lower than the first year. The lifetime consumption LC of the power device is accumulated for an operation of several years considering the panel degradation rate of 0.55% per year, the cumulative life consumption of the power device with and without panel

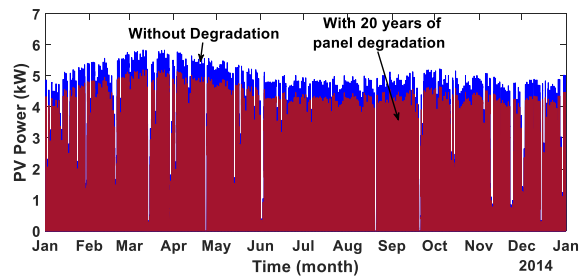
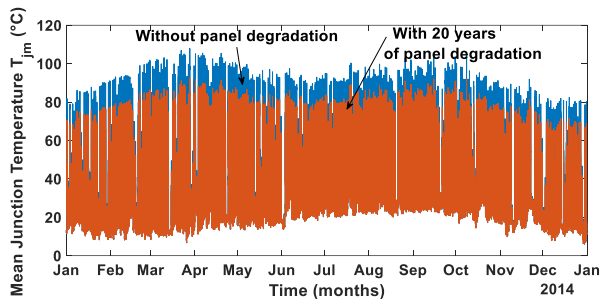
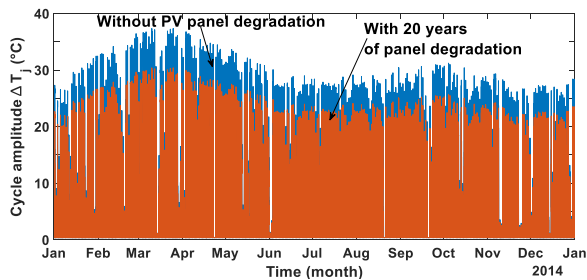


Fig. 20. Available power from PV panels in one year, without degradation, and with 20 years of panel degradation, the PV panels are south oriented and tilt of  $37^\circ$ .



(a)



(b)

Fig. 21. Thermal loading of a single IGBT device in the PV inverter for yearly mission profile data with and without panel degradation: (a) Mean junction temperature  $T_{jm}$  and (b) Cycle amplitude of the junction temperature variation  $\Delta T_j$ .

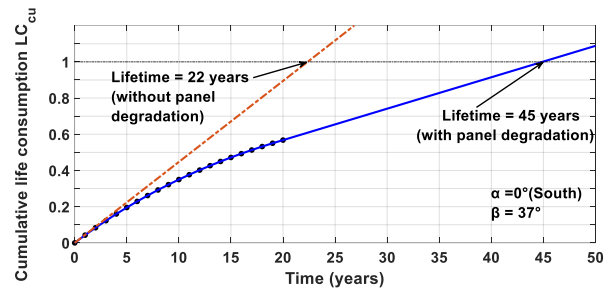


Fig. 22. Cumulative LC of the power device with and without panel degradation.

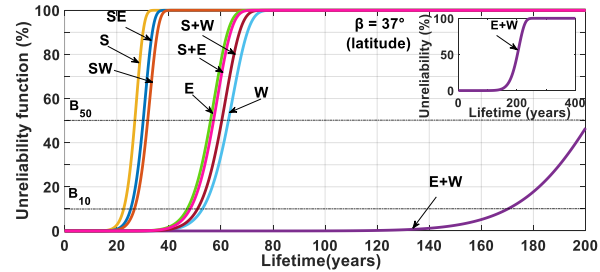


Fig. 23. Unreliability function (Weibull CDF function) of the PV inverter installed in Algeria for different orientations considering PV panel degradation for 20 years.

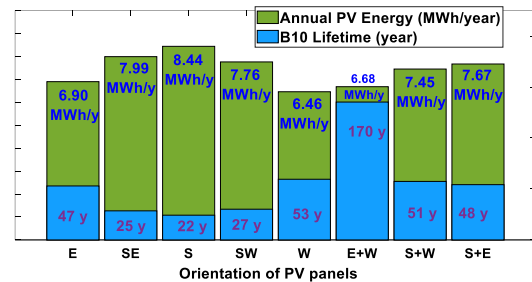


Fig. 24. PV Energy yield and  $B_{10}$  lifetime of the PV inverter installed in Algeria for different tilt angles of PV panels in one year considering PV panel degradation for 20 years.

degradation for the case of south-facing and tilt of  $37^\circ$  is shown in Fig. 22. It can be observed that the lifetime of the power device for this case is near twice the lifetime without considering panel degradation.

As can be seen in Fig. 23 and Fig. 24, the PV inverter lifetime increased considerably compared to Fig. 15 and Fig. 17 where the PV degradation impact is not considered. For most orientations, the inverter lifetime increased by more than 130%. It can be observed from Fig. 17 and Fig. 24, the highest increase in PV inverter lifetime is observed for the south orientation, where  $B_{10}$  is shifted from 8 years to 22 years, which is an increase of 175%. In most cases, it can be said that the inverter replacement is decreased by 50% by considering panel degradation. Hence, the results in this paper agree with the study in [13], where PV panel degradation will result in an overestimation of the maintenance cost for PV inverters in the design phase, given as  $C_{0\&m}$ , the operational and maintenance cost in [11]. This means that PV panel degradation should be considered in the lifetime estimation of PV inverter systems.

## VI. CONCLUSION

In this paper, the impact of PV panel positioning (tilt, orientation) on the PV inverter lifetime is studied, the evaluation is carried out based on the mission profiles of Algiers, Algeria, characterized with a Mediterranean climate. The results reveal that the tilt angle of PV panels alters the energy production slightly. However, its impact on the PV inverter lifetime is very low. On the other hand, the orientation of PV panels has a strong impact on the PV inverter lifetime, where for some orientations the PV energy production is kept high enough and the PV inverter lifetime is increased dramatically. The results presented in this paper can be used to evaluate the design trade-off between the energy yield and PV inverter lifetime for different PV positioning. The methodology given in this paper can be applied for any location with certain mission profile, where the yearly irradiance profile for different tilts and orientations are required as input for the mission profile based lifetime estimation. In this work, the mission profile from Algiers, Algeria is used as a case study to investigate the impact of tilt and orientation angle on the lifetime evaluation of the PV inverter. Besides, the daily irradiance profiles for different tilt and orientation angles, which represent a typical short-term operation of the PV inverter under clear-day condition can be applicable to most locations. In the case of the long-term operation, e.g., one-year, the long-term variation of the mission profile is strongly influenced by the location of the installation. However, the results can in general represent the location with similar climate condition, e.g., moderate climate. For other climate conditions, the same method presented in this paper can still be applied to quantify the impact of PV panel positioning on the inverter reliability. Moreover, according to the results, it is found that PV panel degradation is an important parameter in the estimation of the PV inverter lifetime and needs to be considered in the reliability assessment. More results related to PV panel degradation is a subject of future research.

## ACKNOWLEDGMENT

We would like to express our very great appreciation to Dr Kamel Agroui from Semiconductors Technology for Energetic Research Center (CRTSE), Algiers for his valuable help during this research work, and we would like to give special thanks to Dr. Amar Hadj Arab from CDER (Centre de Développement des Energies Renouvelables), Algiers, Algeria for his help in providing the needed data.

## REFERENCES

- [1] REN21, Paris, France, "Renewables 2017: Global Futures Report (GFR)," 2017. [Online]. Available: <http://www.ren21.net/>.
- [2] F. Blaabjerg, K. Ma and Y. Yang, "Power electronics - The key technology for Renewable Energy Systems," *2014 Ninth International Conference on Ecological Vehicles and Renewable Energies (EVER)*, Monte-Carlo, 2014, pp. 1-11.
- [3] L. Moore and H. Post, "Five years of operating experience at a large, utility-scale photovoltaic generating plant", *Progress in Photovoltaics: Research and Applications*, vol. 16, no. 3, pp. 249-259, 2008.
- [4] F. Blaabjerg, D. Zhou, A. Sangwongwanich and H. Wang, "Design for reliability in renewable energy systems," *2017 International Symposium on Power Electronics (Ee)*, Novi Sad, 2017, pp. 1-6.
- [5] H. Wang et al., "Transitioning to physics-of-failure as a reliability driver in power electronics," *IEEE J. Emerg. Sel. Topics Power Electron.*, vol. 2, no. 1, pp. 97-114, March 2014.
- [6] H. Huang and P. A. Mawby, "A Lifetime Estimation Technique for Voltage Source Inverters," *IEEE Trans. Power Electron.*, vol. 28, no. 8, pp. 4113-4119, Aug. 2013.
- [7] Y. Yang, A. Sangwongwanich and F. Blaabjerg, "Design for reliability of power electronics for grid-connected photovoltaic systems," *CPSS Trans Power Electron. Appl.*, vol. 1, no. 1, pp. 92-103, Dec. 2016.
- [8] T.Y. Hung, C.J. Huang, C.C. Lee, C.C. Wang, K.C. Lu and K.C. Chiang, "Investigation of solder crack behavior and fatigue life of the power module on different thermal cycling period," in *Microelectronic Engineering*, 107, 125-129.
- [9] A. Albarbar, and C. Batunlu, *Thermal Analysis of Power Electronic Devices Used in Renewable Energy Systems*, Springer International Publishing, 2018.
- [10] M. Ciappa, "Selected failure mechanisms of modern power modules," in *Microelectronics reliability* 42.4-5 (2002): 653-667.
- [11] Y. Yang, H. Wang, A. Sangwongwanich, and F. Blaabjerg, "Design for reliability of power electronic systems," in *Power Electronic Handbook* 4th ed. Butterworth-Heinemann. 2018, ch. 45, pp. 1423-1440.
- [12] A. Sangwongwanich, Y. Yang, D. Sera, F. Blaabjerg and D. Zhou, "On the impacts of PV array sizing on the inverter reliability and lifetime," *IEEE Trans. Ind. Appl.*, vol. 54, no. 4, pp. 3656-3667, July-Aug. 2018.
- [13] A. Sangwongwanich, Y. Yang, D. Sera and F. Blaabjerg, "Lifetime evaluation of grid-connected PV inverters considering panel degradation rates and installation sites," *IEEE Trans. Power Electron.*, vol. 33, no. 2, pp. 1225-1236, Feb. 2018.
- [14] Deutsche Gesellschaft für Sonnenenergie, *Planning and Installing Solar Thermal Systems: A Guide for Installers, Architects and Engineers*, Earthscan, 2010.
- [15] A. Kankiewicz, "West vs. south: Why change the orientation of your solar PV system", Clean Power Research, 2019. [Online]. Available: <https://www.cleanpower.com/2015/west-vs-south-pv-system/>. [Accessed: 22-May-2019].
- [16] J. Rhodes, C. Upshaw, W. Cole, C. Holcomb and M. Webber, "A multi-objective assessment of the effect of solar PV array orientation and tilt on energy production and system economics", *Solar Energy*, vol. 108, pp. 28-40, Oct. 2014.
- [17] E. Asl-Soleimani, S. Farhangi and M. Zabih, "The effect of tilt angle, air pollution on performance of photovoltaic systems in Tehran", *Renewable Energy*, vol. 24, no. 3-4, pp. 459-468, Nov. 2001.
- [18] M. Kacira, M. Simsek, Y. Babur and S. Demirkol, "Determining optimum tilt angles and orientations of photovoltaic panels in Sanliurfa, Turkey", *Renewable Energy*, vol. 29, no. 8, pp. 1265-1275, Jul. 2004.
- [19] A. Mraoui, M. Khelif and B. Benyoucef, "Optimum tilt angle of a photovoltaic system: Case study of Algiers and Ghardaia," *2014 5th International Renewable Energy Congress (IREC)*, Hammamet, 2014, pp. 1-6.
- [20] M. Hartner, A. Ortner, A. Hiesl and R. Haas, "East to west – The optimal tilt angle and orientation of photovoltaic panels from an electricity system perspective", *Applied Energy*, vol. 160, pp. 94-107, Dec. 2015.
- [21] A. Lahnaoui, P. Stenzel and J. Linssen, "Tilt Angle and Orientation Impact on the Techno-economic Performance of Photovoltaic Battery Systems", *Energy Procedia*, vol. 105, pp. 4312-4320, May. 2017.
- [22] A. Kankiewicz, "West vs. south: Why change the orientation of your solar PV system", Clean Power Research, 2019. [Online]. Available: <https://www.cleanpower.com/2015/west-vs-south-pv-system/>. [Accessed: 22-May-2019].
- [23] Y. Yang, H. Wang, F. Blaabjerg, and K. Ma, "Mission profile based multi-disciplinary analysis of power modules in single-phase transformerless photovoltaic inverters," in *Proc. Eur. Conf. Power Electron. Appl.*, Sep. 2013, pp. 1-10.
- [24] Single-Phase, Grid-Connected PV Inverter (Lookup Table-Based PV Cell, dP/dV MPPT) | Plexim, Plexim.com, 2019. [Online]. Available: <https://www.plexim.com/support/application-examples/281>. [Accessed: 23-Oct-2019].



[25] Infineon.com, 2019. [Online]. Available: [https://www.infineon.com/dgdl/Infineon-IKW30NG0H3-DS-v02\\_02-en.pdf?fileId=db3a3043266237920126bc80c5f041c9](https://www.infineon.com/dgdl/Infineon-IKW30NG0H3-DS-v02_02-en.pdf?fileId=db3a3043266237920126bc80c5f041c9). [Accessed: 23-Oct-2019].

[26] J. Duffie and W. Beckman, *Solar Engineering of Thermal Processes*, Somerset: Wiley, 2013.

[27] Estimating solar radiation according to semi empirical approach of PERRIN DE BRICHAMBAUT: application on several areas with different climate in Algeria

[28] M.R. Yaiche, A. Bouhanik, S. Bekkouche, A. Malek and T. Benouaz, "Revised solar maps of Algeria based on sunshine duration", *Energy Conversion and Management*, vol. 82, pp. 114-123, Jun. 2014.

[29] B. Liu and R. Jordan, "Daily insolation on surfaces tilted towards equator," *ASHRAE J.*, vol. 10, pp. 53-59, 1961.

[30] M.R. Yaiche and S. M. A. Bekkouche, "Estimation du rayonnement solaire global en Algérie pour différents types de ciel." *Revue des Energies Renouvelables*, vol. 13, no 4, pp. 683-695, Dec. 2010.

[31] A. H. Arab, Y. Bakelli, S. Semaoui, F. Bandou and I. H. Mohammed, "Long term performance of crystalline silicon photovoltaic modules," *2015 3rd International Renewable and Sustainable Energy Conference (IRSEC)*, Marrakech, 2015, pp. 1-5.

[32] K. Agroui, "Indoor and Outdoor Characterizations of Photovoltaic Module Based on Mulicrystalline Solar Cells", *Energy Procedia*, vol. 18, pp. 857-866, 2012.

[33] V. Sharma and S. Chandel, "Performance and degradation analysis for long term reliability of solar photovoltaic systems: A review", *Renewable and Sustainable Energy Reviews*, vol. 27, pp. 753-767, Nov 2013.

[34] A. Skoczek, T. Sample and E. Dunlop, "The results of performance measurements of field-aged crystalline silicon photovoltaic modules", *Progress in Photovoltaics: Research and Applications*, vol. 17, no. 4, pp. 227-240, Dec 2009.

[35] O. Sastry et al., "Performance analysis of field exposed single crystalline silicon modules", *Solar Energy Materials and Solar Cells*, vol. 94, no. 9, pp. 1463-1468, Sep 2010.

[36] K. Agroui, M. Jaunich and A. Arab, "Analysis Techniques of Polymeric Encapsulant Materials for Photovoltaic Modules: Situation and Perspectives", *Energy Procedia*, vol. 93, pp. 203-210, 2016.

[37] K. Agroui, G. Collins, F. Giovanni and W. Stark, "A Comprehensive Indoor and Outdoor Aging of the Cross-Linked EVA Encapsulant Material for Photovoltaic Conversion", *Polymer-Plastics Technology and Engineering*, vol. 54, no. 7, pp. 719-729, 2015.

[38] K. Agroui, "Encapsulation and Analysis Techniques of Crystalline and Emerging Photovoltaic Modules Technologies: Algerian Experience," *2018 International Conference on Communications and Electrical Engineering (ICCEE)*, El Oued, Algeria, 2018, pp. 1-7.

[39] M. Vázquez and I. Rey-Stolle, "Photovoltaic module reliability model based on field degradation studies", *Progress in Photovoltaics: Research and Applications*, vol. 16, no. 5, pp. 419-433, Mar. 2008.

[40] M. Köntges, S. Kurtz, C. Packard, U. Jahn, K. A. Berger, K. Kato, T. Friesen, H. Liu, M. Van Iseghem, J. Wohlgemuth, D. Miller, M. Kempe, P. Hacke, F. Reil, N. Bogdanski, W. Herrmann, C. Buerhop-Lutz, G. Razongles, and G. Friesen, *Review of Failures of Photovoltaic Modules*. IEA, 2014.

[41] D. Jordan, T. Silverman, B. Sekulic and S. Kurtz, "PV degradation curves: non-linearities and failure modes", *Progress in Photovoltaics: Research and Applications*, vol. 25, no. 7, pp. 583-591, Sept. 2016.

[42] M. Matsuishi and T. Endo, "Fatigue of metals subjected to varying stress," *Jap Soc. Mech. Eng.*, Fukouka, Japan, Mar. 1968.

[43] U. Scheuermann and R. Schmidt, "Impact of load pulse duration on power cycling lifetime of Al wire bonds", *Microelectronics Reliability*, vol. 53, no. 9-11, pp. 1687-1691, Sep. 2013.

[44] U. Scheuermann, R. Schmidt and P. Newman, "Power cycling testing with different load pulse durations," *7th IET International Conference on Power Electronics, Machines and Drives (PEMD 2014)*, Manchester, 2014, pp. 1-6.

[45] P. D. Reigosa, H. Wang, Y. Yang and F. Blaabjerg, "Prediction of bond wire fatigue of IGBTs in a PV inverter under a long-term operation," *IEEE Trans. Power Electron.*, vol. 31, no. 10, pp. 7171-7182, Oct. 2016.

[46] P. O'Connor and A. Kleyner, *Practical Reliability Engineering*, John Wiley & Sons, 2012.

[47] S. Bouguerra, K. Agroui, O. Gassab, A. Sangwongwanich and F. Blaabjerg, "Lifetime Estimation and Reliability of PV Inverter With Multi-Timescale Thermal Stress Analysis," *2019 International Aegean Conference on Electrical Machines and Power Electronics (ACEMP) & 2019 International Conference on Optimization of Electrical and Electronic Equipment (OPTIM)*, Istanbul, Turkey, 2019, pp. 402-408.

[48] ZVEL, "How to measure lifetime for robustness validation - step by step," Rev. 1.9, Nov. 2012.



Sara Bouguerra (S'19) was born in Algiers, Algeria, in May. 01, 1993. She received the B.Sc. degree in electrical and electronic engineering and the M.Sc. degree in Telecommunications in 2014 and 2016, respectively from the Institute of Electrical and Electronic Engineering IGEE, Boumerdes, Algeria, where she is currently working toward the Ph.D. degree in Electrical Engineering. She was a guest Ph.D. student in Aalborg University in Denmark from September to November 2019.

Her research interests include PV system design and sizing, Reliability of PV modules and PV inverters. She is also interested in the fields of telecommunications and electromagnetic compatibility (EMC).



Mohamed Rédha Yaiche research engineer advisor in the Development Center of Renewable Energies, CDER Bouzaréah (Algiers-Algeria), and his present research activities are in the area of the potential solar in Algeria. He is interested in the influence of various radiometric parameters on solar systems performance for different types of sky. Many codes have been conceived and developed in the EXCEL language to adopt several theoretical approaches. These computer codes are the most complete range for creating conversational interfaces. It reduces the execution time, and allows users to better understand the information and react quickly. He has about 31 years of research experience and he has published many related articles in this field.



Oussama Gassab (S'17) was born in Djelfa, Algeria, in Feb. 14, 1990. He received the B.Sc. degree in electrical and electronic engineering and the M.Sc. degree in telecommunications from the National Institute of Electrical and Electronic Engineering (IGEE), Boumerdes, Algeria, in 2013 and 2015, respectively, where he is working toward Ph.D. in antenna array design. He is currently working toward another Ph.D. degree in electromagnetic compatibility (EMC) at Shanghai Jiao Tong University, Shanghai, China.

His research interests include electromagnetic compatibility, antenna array design, distributed-parameter circuit modeling, statistical models for the characterization of interference effects, and shielding. He is also interested in the fields of power electronics, mathematics, and modern physics.



Ariya Sangwongwanich (S'15-M'19) received the M.Sc. and Ph.D. degree in energy engineering from Aalborg University, Denmark, in 2015 and 2018, respectively. Currently, he is working as a Postdoc Fellow at the Department of Energy Technology, Aalborg University.

He was a Visiting Researcher with RWTH Aachen, Aachen, Germany from September to December 2017. His research interests include control of grid-connected converter, photovoltaic systems, reliability in power electronics and multilevel converters. He has co-



authored the book – Advanced in Grid-Connected Photovoltaic Power Conversion Systems. In 2019, he received the Danish Academy of Natural Sciences' Ph.D. prize and the Spar Nord Foundation Research Award for his Ph.D. thesis.



**Frede Blaabjerg** (S'86–M'88–SM'97–F'03) was with ABB-Scandia, Randers, Denmark, from 1987 to 1988. From 1988 to 1992, he got the PhD degree in Electrical Engineering at Aalborg University in 1995. He became an Assistant Professor in 1992, an Associate Professor in 1996, and a Full Professor of power electronics and drives in 1998. From 2017 he became a Villum Investigator. He is honoris causa at University Politehnica Timisoara (UPT), Romania and Tallinn Technical University (TTU) in Estonia.

His current research interests include power electronics and its applications such as in wind turbines, PV systems, reliability, harmonics and adjustable speed drives. He has published more than 600 journal papers in the fields of power electronics and its applications. He is the co-author of four monographs and editor of ten books in power electronics and its applications.

He has received 32 IEEE Prize Paper Awards, the IEEE PELS Distinguished Service Award in 2009, the EPE-PEMC Council Award in 2010, the IEEE William E. Newell Power Electronics Award 2014, the Villum Kann Rasmussen Research Award 2014, the Global Energy Prize in 2019 and the 2020 IEEE Edison Medal. He was the Editor-in-Chief of the IEEE TRANSACTIONS ON POWER ELECTRONICS from 2006 to 2012. He has been Distinguished Lecturer for the IEEE Power Electronics Society from 2005 to 2007 and for the IEEE Industry Applications Society from 2010 to 2011 as well as 2017 to 2018. In 2019-2020 he serves a President of IEEE Power Electronics Society. He is Vice-President of the Danish Academy of Technical Sciences too.

He is nominated in 2014-2019 by Thomson Reuters to be between the most 250 cited researchers in Engineering in the world.